Supporting Information

Gan *et al.* 10.1073/pnas.0808035105

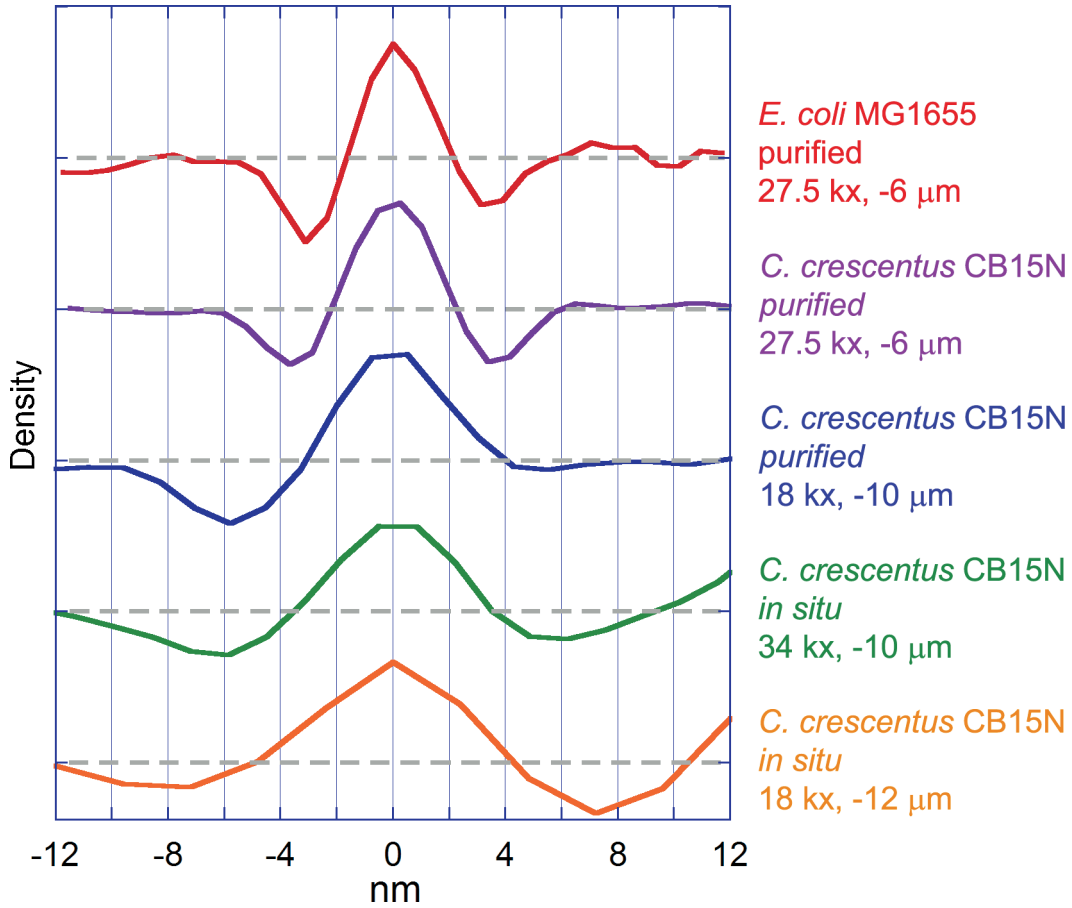

Fig. S1. Density profiles (arbitrary units) across sacculi side walls. In situ profiles were taken from whole-cell tomograms (Fig. 2*A*) and in vitro profiles were taken from purified sacculus tomograms (Fig. 2*B*). The plots are centered on the middle of the peptidoglycan side wall. The gray dotted line is the density of the buffer. The density dips are Fresnel fringes that are generated by the defocus (−6, −10, or −12 μm) used to generate image contrast. Note that the density shoulders rising on the right side of the in situ plots correspond to the inner membrane. Three known artifacts make the sacculus appear thicker here than it is, making these measurements upper limits of the real width. First, the defocus spreads the density, so that the apparent 4-nm thickness is an ''upper'' limit. Second, the images could not be segmented perfectly, which introduces errors in the determination of the exact center of the sacculus side wall, which in turn leads to blurring of the edges in the profile. Third, the plots of the in situ sacculi include the densities of peptidoglycan-embedded proteins, which extend beyond the sacculus. We conclude that the sacculus is no more than 4-nm thick.

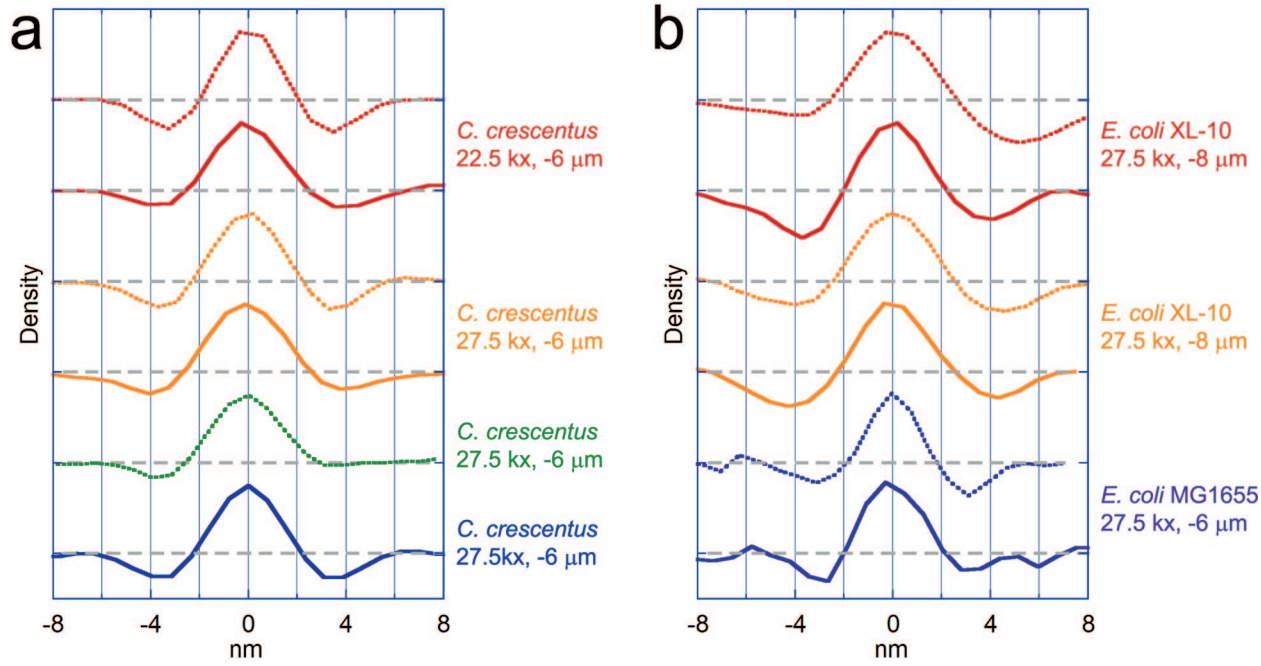

Fig. S2. Density profiles at different positions around the sacculus. Additional density profiles were taken from the best four *C. crescentus* (*A*) and three *E. coli* (*B*) sacculi tomograms. Each color represents a different sacculus. The solid profiles were taken from the side wall; the dotted profiles were taken from either the stalk (*C. crescentus*) or the pole (*E. coli*). In (*A*), the tomogram used for the green dotted profile did not show the side wall, whereas the tomogram used for the blue profile did not show enough stalk for segmentation. The orange trace in (*A*) and the violet trace in Fig. S1 were generated by using the same tomogram.

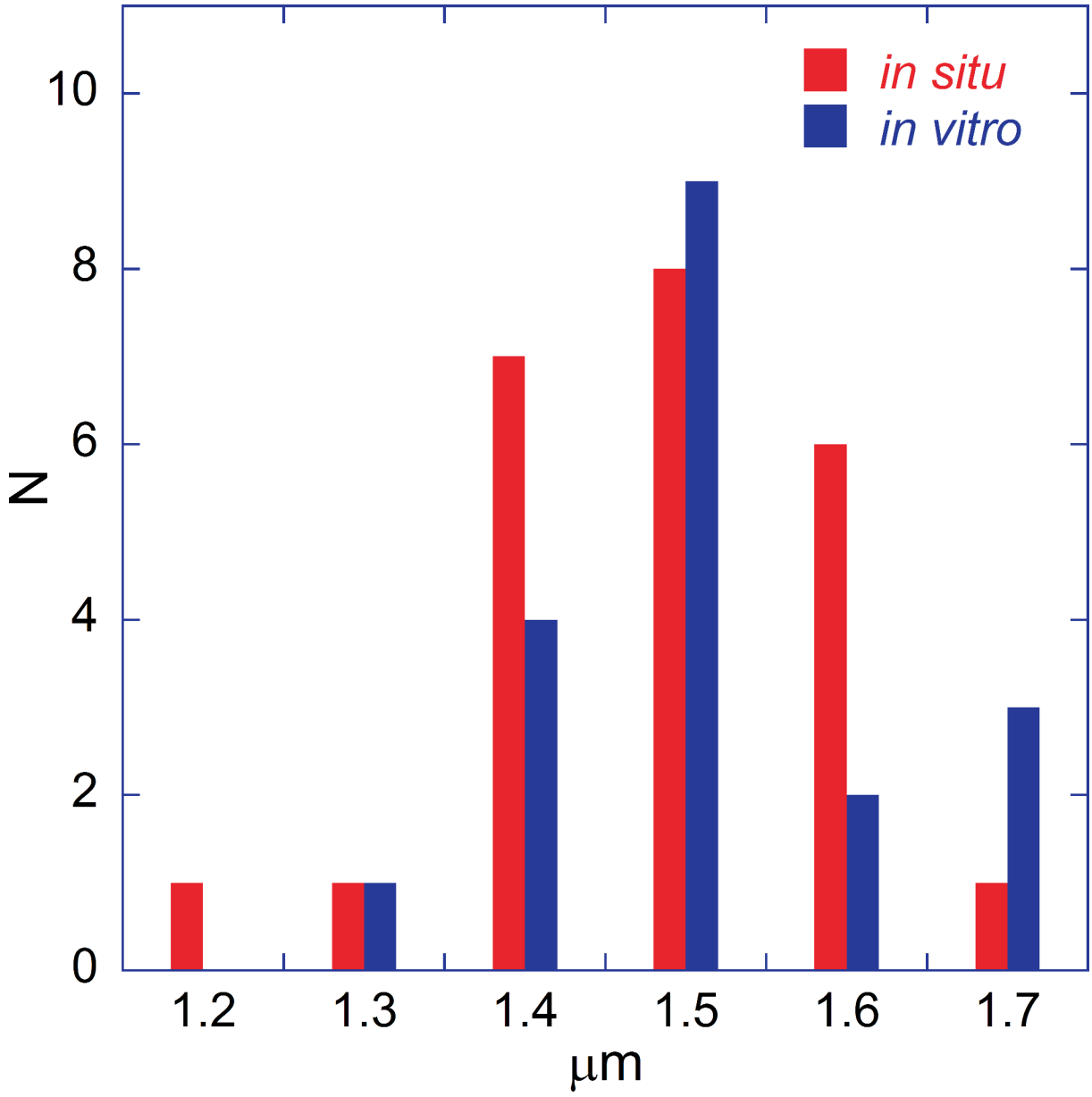

Fig. S3. Sacculi circumferences. The measurements were taken from tomograms of either intact *C. crescentus* CB15N cells (*in situ*) or purified sacculi (*in vitro*). No statistically significant difference in the mean circumferences was detected with an unpaired, two-tailed *t* test.

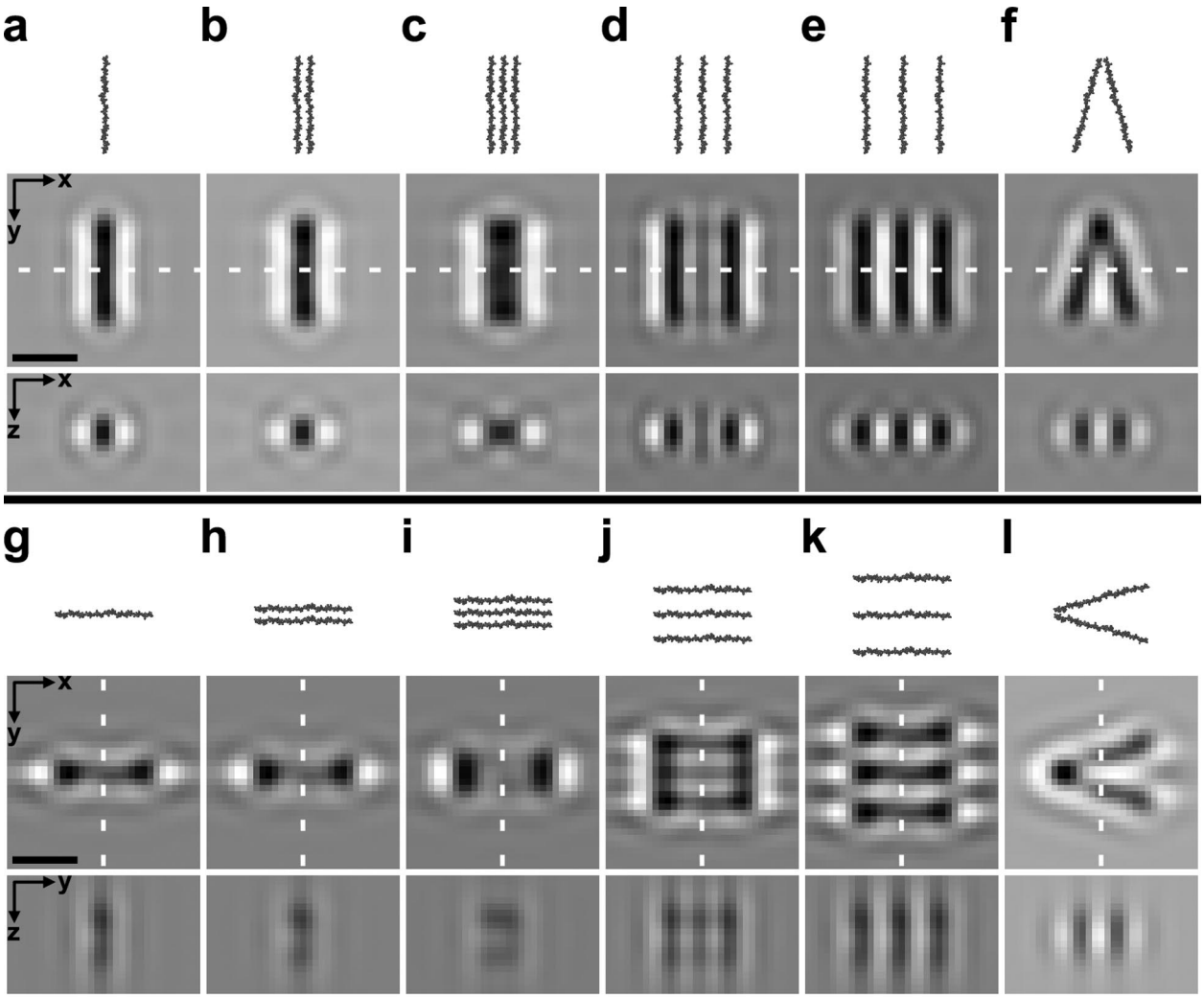

Fig. S4. Simulated tomograms of glycan strands Glycan strands (18-mers) were aligned either parallel (*a–f*) or perpendicular (*g–l*) to the tilt axis, which runs up and down. The glycan strands have center-to-center separations of 2 nm (*b*, *h*, *c*, *i*), 4 nm (*d*, *j*), and 6 nm (*e*, *k*). The pairs of glycan strands in *f* and *l* are offset by a 30 ° rotation. Tilt series with 6-μm defocus and 0.96-nm pixel size were simulated by simple projection, and then 3-D reconstructed with IMOD just as for the experimental data. (*Top*) Space-filling input model. (*Middle*) Central z-slice (parallel to *x* and *y* axes) of simulated tomogram. (*Bottom*) Cross-sections cut along the dashed line in the middle panel, parallel to the x-z plane (*a–f*) or the y-z plane (*g–l*). Note that the cross-sections show that single glycan strands are highly enlongated along the *z* axis, which recapitulates the oblong glycan densities seen in Movies S1 and S2. We conclude that the imaging conditions would in fact allow even thin glycan strands to be resolved, if they were spaced by at least 4 nm. (Scale bar, 10 nm.)

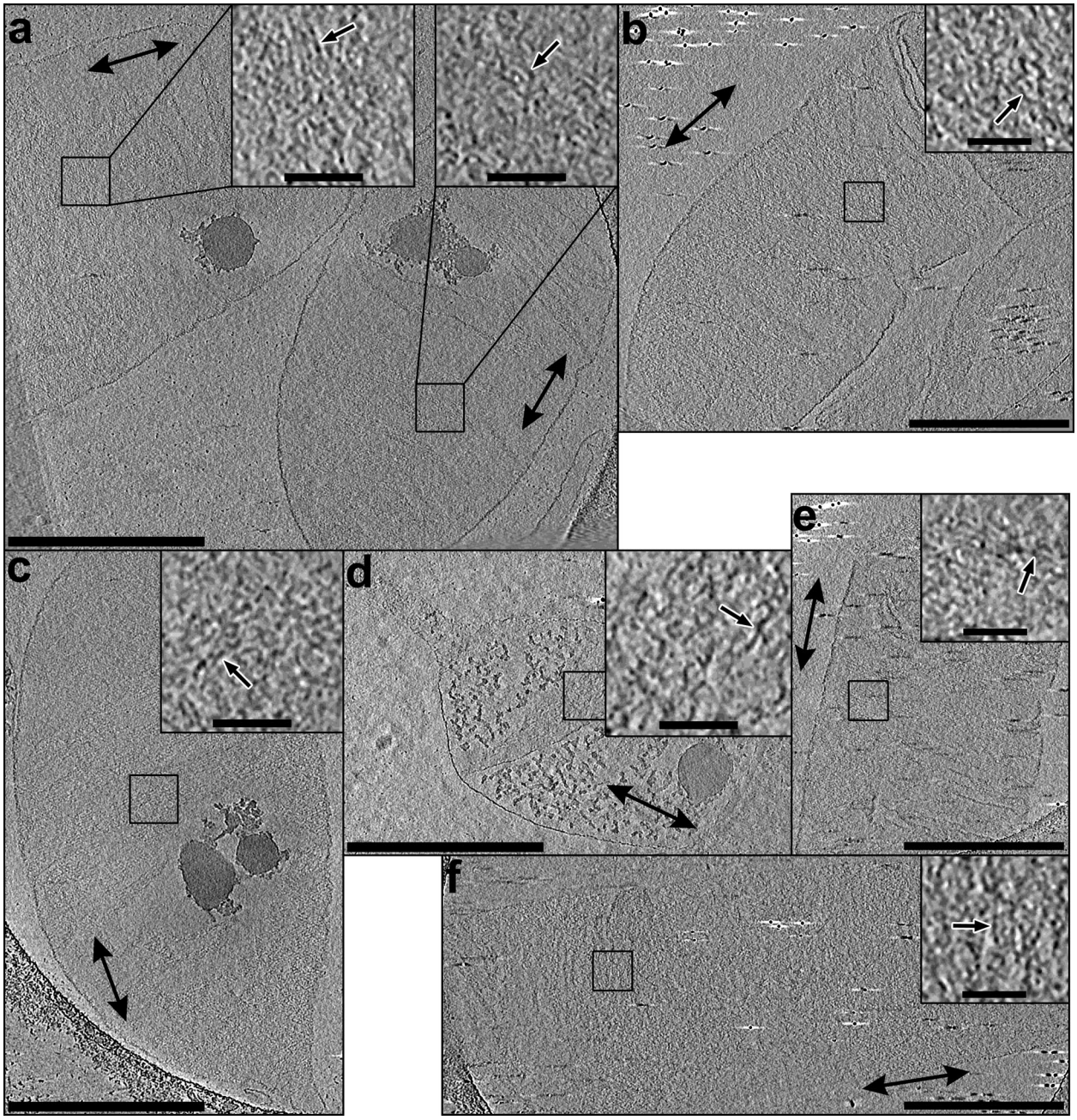

Fig. S5. Examples of *C. crescentus* sacculi. Ten-nm thick Z-slices of *C. crescentus* CB15N sacculi. The double-headed arrow denotes the sacculus polar axis. *Insets* show four-fold enlarged views of the boxed region; the arrowheads point to glycan strands. Note that glycan strands are visible in all cases, regardless of the orientation of the sacculus with respect to the tilt axis, which is vertical here. The glycan strand densities are therefore reproducible and are not artifacts caused by the missing wedge. (Large scale bars, 500 nm; *Inset* scale bars, 50 nm.)

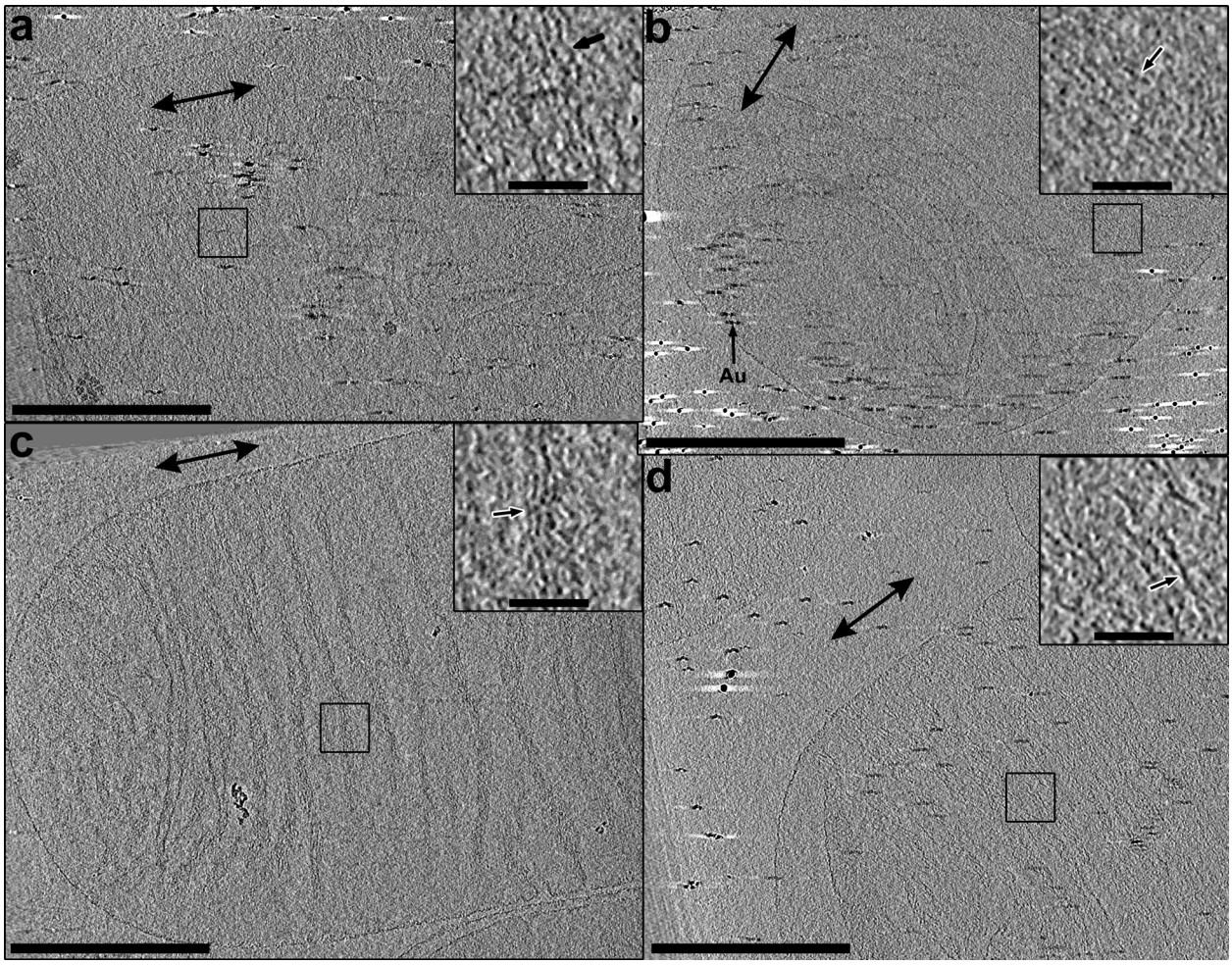

Fig. S6. Examples of *E. coli* sacculi. Ten-nm thick Z-slices of sacculi from *E. coli* strains MG1655 (*A* and *B*) and XL-10 (*C* and *D*). The labels and scale bars are identical to those in Fig. S5. The sacculus in (*C*) is the same as shown in Fig. 3*B*.

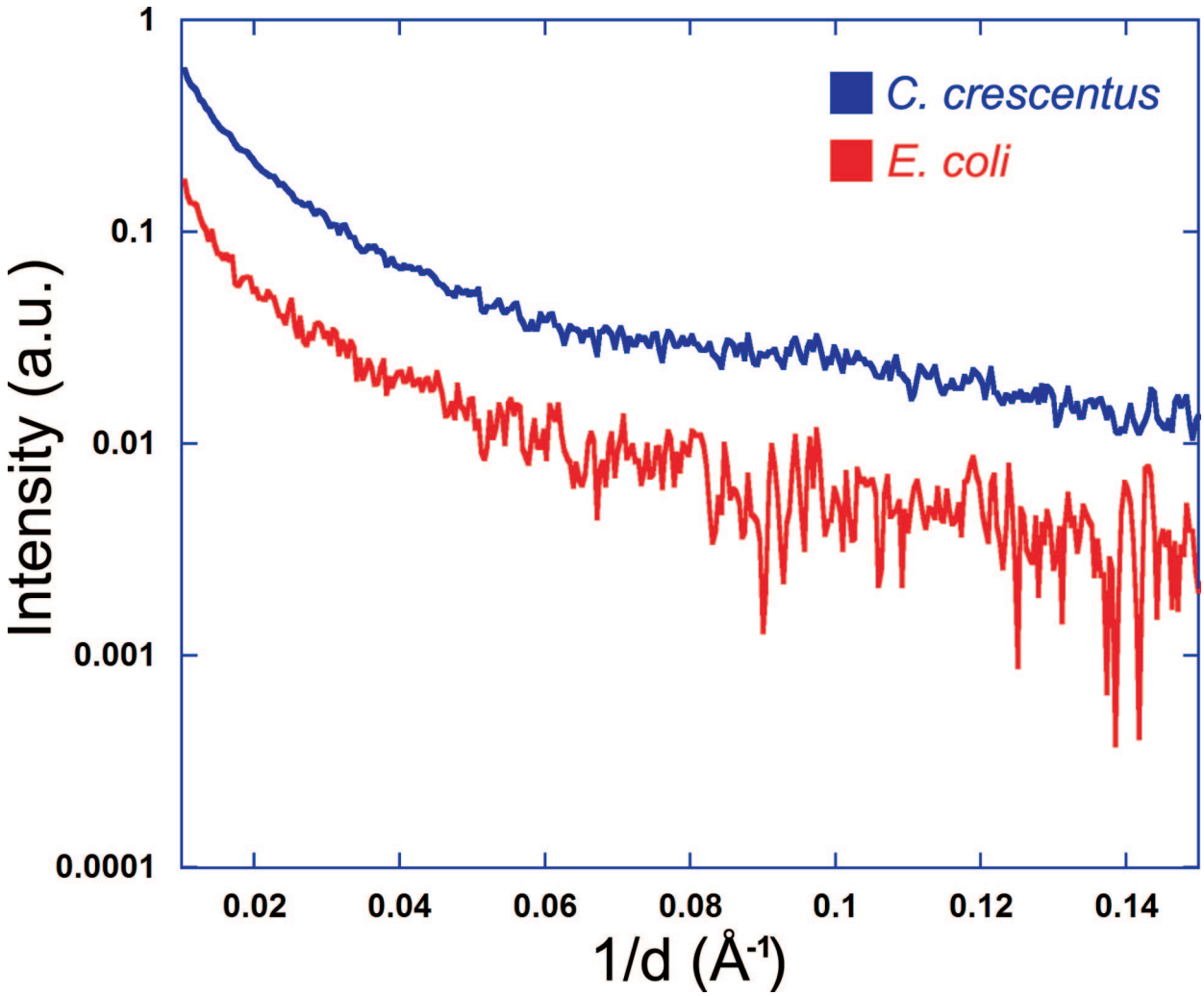

Fig. S7. Small angle X-ray scattering of sacculus solutions. SAXS patterns of *C. crescentus* and *E. coli* sacculi show no dominant peaks.

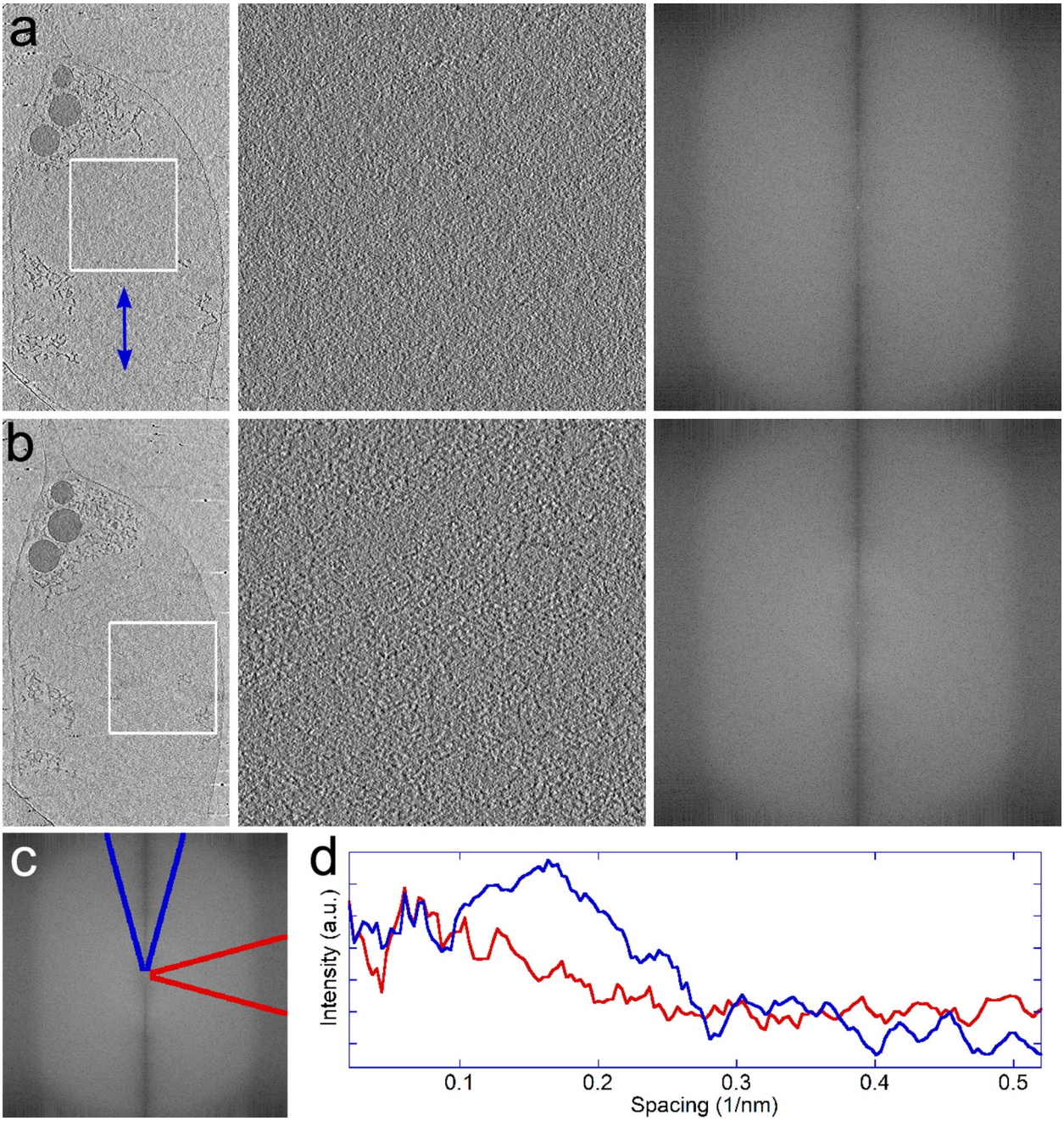

Fig. S8. Fourier analysis of a *C. crescentus* sacculus. Regions that were 512 × 512 (*Insets* in *Left Images*) were selected from the (*A*) lumen (a ''control'' region) and (*B*) through the ''upper'' half of the sacculus from Fig. 2*B*. The double-headed blue arrow in the *Left Image* of (*A*) indicates the sacculus polar axis. The tilt axis runs up and down. Close-ups (*A* and *B*, *Middle Images*) reveal that the lumen, which contains only buffer, lacks the individual strands seen within the wall, which we have interpreted as glycan strands. The power spectra (*A* and *B*, *Right Images*) reveal that the lumen is featureless, but the sacculus has a broad range of spacings (see brighter ellipsoidal region in the center extending to about one-third Nyquist frequency vertically and one-fourth Nyquist horizontally; see below). Because no sharp rings were detected, the glycan strands are not crystalline. These results are similar to and confirm previous small angle X-ray scattering experiments done by others and repeated in this work, but specific regions of 3-D tomograms of individual sacculi could be transformed here, so the power spectra could be averaged over 30° wedges delimited by the blue and red wedges in (*C*), which run parallel and perpendicular to the polar axis, respectively. A 1-D plot (*D*) of the background-subtracted (sacculus minus lumen) power spectra wedges reveals that the strands are more often perpendicular to the polar axis of the cell than parallel. This is not an artifact of the missing wedge or tilt axis, because a similar result was obtained from a sacculus lying approximately perpendicular to the tilt axis.

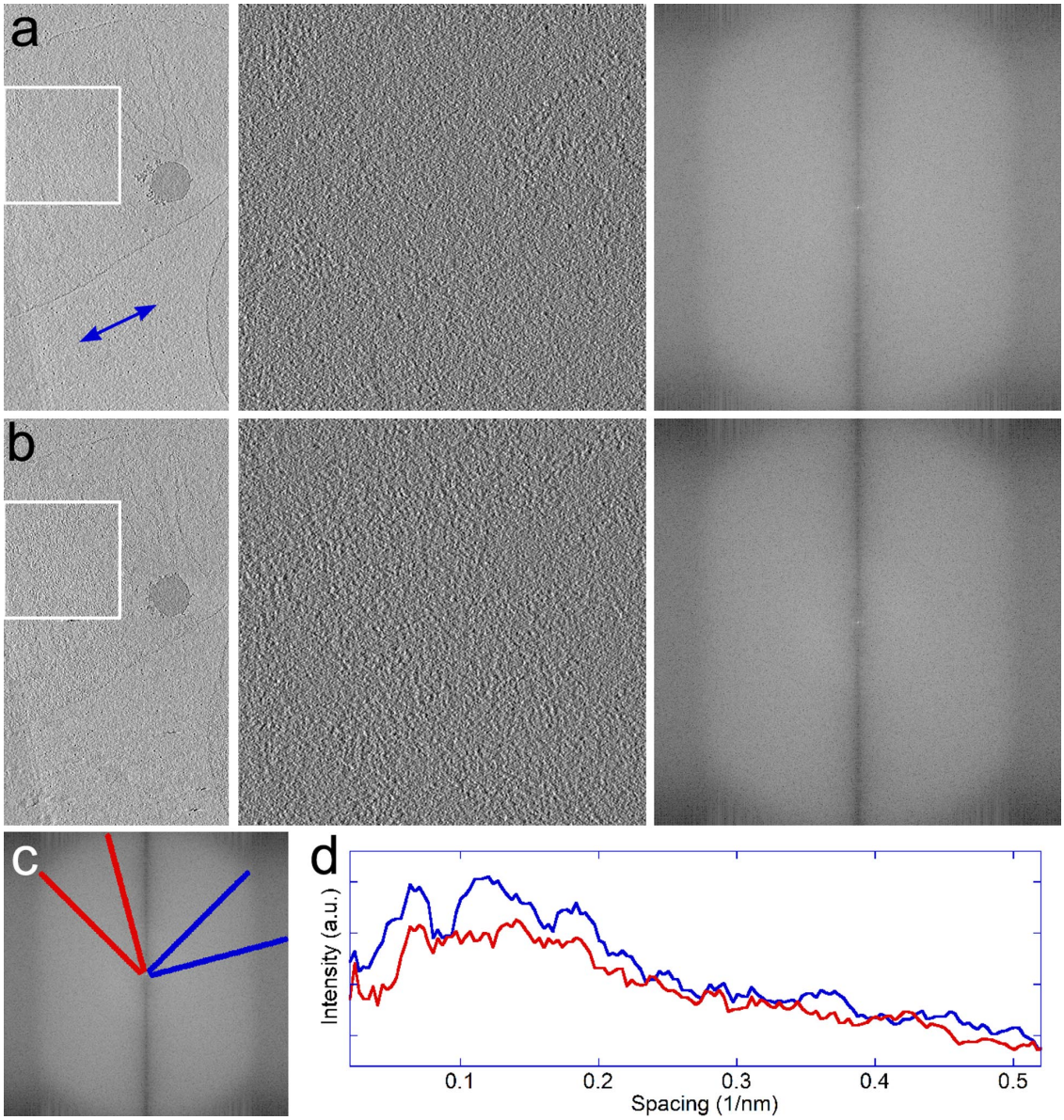

Fig. S9. Fourier analysis of another *C. crescentus* sacculus. The labels are the same as for Fig. S8. This tomogram (from Fig. S5*A*) has less contrast than the tomogram in Fig. S8 and this sacculus is more crumpled such that some sacculus densities are observable in the ''lumen'' slice. Both of the preceding properties attenuate the differences between the 1-D power spectra (*D*) taken (blue) parallel and (red) perpendicular to the sacculus polar axis. Note that the power is greater in the direction parallel to the sacculus polar axis rather than in the direction perpendicular to the sacculus polar axis, just like in Fig. S8. Therefore, the glycans are poorly ordered and not reinforced by the missing wedge, which runs up and down in the figure.

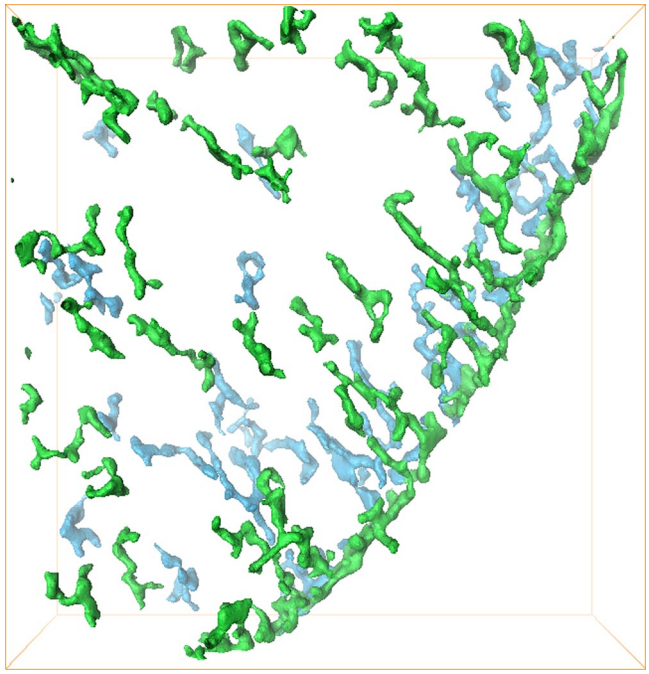

Movie. S1. Molecular architecture of Gram-negative sacculi *C. crescentus*.

Movie S1 (MOV)

Start Time–End Time	Narration
00:02–00:14	01. This is a *Caulobacter crescentus* sacculus tilt series. 02. There are two sacculi stacked on top of each other. 03. The two sacculi are outlined by purple and green dotted lines.
00:21–00:36	04. This is a slice-by-slice view of the tomogram. 05. The two sacculi are outlined by purple and green dotted lines. 06. The sacculi were flattened, so they appear wider than intact cells.
00:43–00:51	07. Here is a close-up view of the tomogram near the side wall of the sacculus on the right. 08. The legend in the lower right corner shows with the orange box where we are looking.
00:53–00:57	09. This is a slice-by-slice view near the collapsed part of the side wall.
00:57–01:07	10. A close-up of the side wall cross-section shows a single line of discrete, punctate densities, which have been interpreted as individual glycan strands, revealing that the sacculus is single-layered.
01:11–01:15	11. This is an isosurface with the shortest and smallest density islands removed.
01:16–01:28	12. Here, the isosurface is shown from two perspectives. 13. The top panel is viewed along the tilt axis, which is roughly parallel to the saccular polar axis. 14. The bottom panel is viewed from above the sacculus surface.
01:29–01:50	15. To simplify the peptidoglycan densities, only a thin cross-section of the sacculus is shown. 16. As the cross-section is translated along the tilt axis, the wrinkled nature of the sacculus becomes apparent. The green- and dark-blue- colored densities are equivalent, reflecting simply how the visualization software renders inside and outside surfaces in these cut-aways.
01:58–02:03	17. To further analyze the morphology of individual strands, all but densest are removed.
02:08–02:34	18. Here, green and light-blue colors have been used to distinguish the "top" and "bottom" halves of the sacculus. 19. The strand densities have been interpreted as glycan strands and have an oval cross-section as expected because of the point spread function of the imaging system. 20. Details of the glycans like bumps, branches and kinks cannot be interpreted at the current resolution and do not reflect their conformations in an intact cell because the sacculi are collapsed.
02:41–02:52	21. An atomic model of a 9-subunit glycan chain has been placed in the density for a sense of scale. 22. Note that because of the imaging and reconstruction parameters used, the density tubes are expected to appear wider than the model.

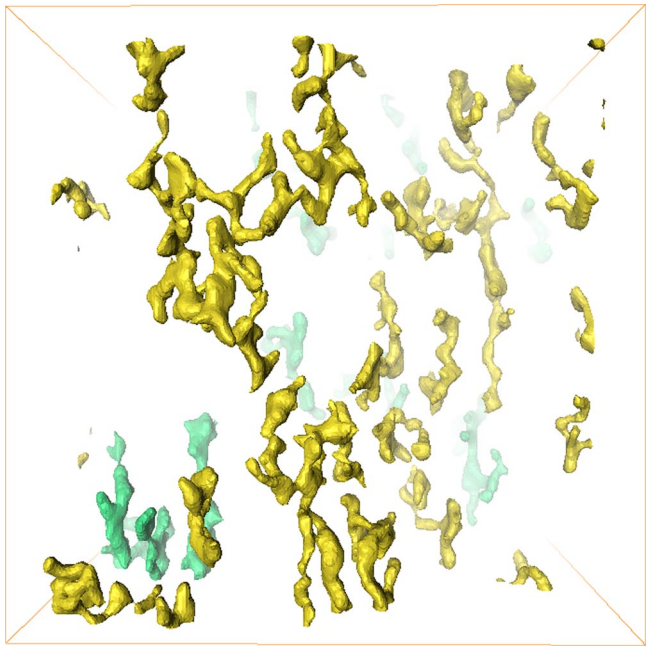

Movie S2. Molecular architecture of Gram-negative sacculi *E. coli*.

Movie S2 (MOV)

Start Time–End Time	Narration
00:02–00:12	01. This is an *E. coli* sacculus tilt series. 02. In the zero-tilt image, the sacculus is outlined by a yellow dotted line.
00:19–00:30	03. This is a slice-by-slice view of the tomogram. 04. The sacculus is outlined by a yellow dotted line. 05. The sacculus is flattened, so it appears wider than an intact cell.
00:34–00:42	06. Here is a slice-by-slice close-up view of the sacculus. 07. Each slice is a 6-nm thick average.
00:49–00:58	08. Here the densities are shown as isosurfaces. 09. Only the strongest and longest density tubes were included in the isosurface for clarity.
01:00–01:08	10. The isosurface is rotated to present a view perpendicular to the sacculus long axis. 11. Note that after collapsing, the sacculus appears corrugated.
01:12–01:20	12. Here, the slice-by-slice close-up is shown below the isosurface. 13. Each slice corresponds to a projection of the densities highlighted in solid red.
01:21–01:27	14. The projected slice and the corresponding isosurface densities are concurrently translated from the "bottom" to the "top" of the tomogram.
01:27–01:41	15. Because the sacculus is corrugated, only strips of the sacculus are visible in any given slice, with buffer in between. 16. In this particular slice, the strips of sacculus are boxed in red, and the intervening low-density buffer is boxed in yellow.
01:57–02:29	17. This is a closer view of the sacculus. 18. Here, yellow and green colors have been used to distinguish the "top" and "bottom" halves of the sacculus. 19. Details of the glycans like bumps, branches and kinks cannot be interpreted at the current resolution and do not reflect their conformations in an intact cell because the sacculi are collapsed. 20. The thin, tube-like glycan strands have an oval cross-section as expected because of the point spread function of the imaging system.